Наносистеми, наноматеріали, нанотехнології
Nanosistemi, Nanomateriali, Nanotehnologii
2025, т. 23, № 3, сс. 719–732
https://doi.org/10.15407/nnn.23.03.0719

PACS numbers: 78.20.Ci, 78.20.Jq, 78.40.Ha, 78.66.Li, 78.67.Bf, 81.20.Fw, 81.40.Tv

High Optical Transmittance of TiO_2 Thin Films Prepared by Sol–Gel Coating Technique

Fouad Zuhair Razzooqi[1], Mohammed S. Radhi[2], Hayder Abbas Sallal[3], and Zainab Al-Khafaji[4,5]

[1]*Al-Qasim Green University,*
Al-Qasim District, Babylon Governorate,
51013 Babylon, Iraq
[2]*College of Materials Engineering,*
Ceramic and Building Materials Department,
University of Babylon,
Hillah, Iraq
[3]*College of Engineering,*
Department of Prosthetics and Orthotics Engineering,
Al-Nahrain University,
Jadriya, Baghdad, Iraq
[4]*Faculty of Engineering and Built Environment,*
Department of Civil Engineering,
Universiti Kebangsaan Malaysia,
43600 UKM Bangi, Selangor, Malaysia
[5]*Imam Ja'afar Al-Sadiq University,*
Qahira, Baghdad, Iraq

In this paper, thin titanium-dioxide films are prepared with sol–gel processing, and the effect of annealing-temperature variations on some optical properties (n, k, d) is investigated. Thin films are determined using the ellipsometry technique, considering the effect of annealing temperatures of 360°C, 460°C, 550°C, and 700°C. By using a spectrophotometer (UV–Vis), the optical properties are determined. As found, the best values of optical transmittance are obtained for the annealed film at 500°C (the spectrophotometric curve at issue is showing the largest transmittance of the visible length, reaching between 80% and 90% at wavelengths ranging from 400 nm to 600 nm, respectively). The best values of reflectance and refractive index appear at $T = 460$°C and $T = 500$°C, as the films show low reflectance values in the visible region 400–700 nm. It should be noted that the annealed film at a temperature of 500°C is the best. All films have a wide band gap of $\cong 3.2$ eV as obtained for all samples prepared, especially, at $T = 500$°C.

У цій роботі було одержано тонкі плівки діоксиду Титану за золь–ґель-технологією. Досліджено вплив зміни температури відпалу на деякі оптичні властивості (n, k, d). Тонкі плівки визначали за допомогою методу еліпсометрії, враховуючи вплив температур відпалу у 360°C, 460°C, 550°C і 700°C. За допомогою спектрофотометра (UV–Vis) було визначено оптичні властивості; було виявлено, що найкращі значення оптичного пропускання було одержано для плівки, відпаленої за 500°C (спектрофотометрична крива показує найбільше пропускання видимого діяпазону, що досягається між 80% і 90% на довжинах хвиль у діяпазоні від 400 нм до 600 нм відповідно). А найкращі значення коефіцієнта відбивання та показника заломлення спостерігаються за $T = 460$°C і $T = 500$°C, оскільки плівки показали низькі значення коефіцієнта відбивання у видимому діяпазоні 400–700 нм. Слід зазначити, що плівка, відпалена за температури у 500°C, є найліпшою. Всі плівки мають широку заборонену зону у $\cong 3{,}2$ еВ, одержану для усіх підготовлених зразків, особливо за $T = 500$°C.

Key words: sol–gel processing, thin films, optical transmittance.

Ключові слова: золь–ґель-оброблення, тонкі плівки, оптичне пропускання.

(Received 8 March, 2024)

1. INTRODUCTION

Titanium dioxide is a solid substance that is white in colour. It is known for its thermal stability, non-flammability, poor solubility, and low cost. Additionally, it is a non-toxic material, which exhibits excellent semiconducting properties. The materials' lack of response to visible light, due to its band gap of 3.2 eV [1–4], allows it to only absorb light in the near ultraviolet range. As a result, the films made from this material exhibit high levels of transparency in the visible region [5, 6].

Titanium dioxide finds extensive application in a wide array of consumer goods and industrial sectors, including the treatment of various surfaces [7]. Scientists are highly enthusiastic about the wide range of applications that can be achieved with this field. These include photocatalytic processes, solar cells, gas sensors, antireflective coatings, and electrochromic systems [8]. Various methods have been employed to create thin films of TiO_2, such as e-beam evaporation, chemical vapour deposition, sputtering, spray pyrolysis, photodeposition, sol–gel processing, and hydrothermal method.

Nanostructure films made using sol–gel spin coating exhibit exceptional optical properties that make them ideal for use in solid-state photovoltaic solar cells. The optical characteristics of TiO_2 films under visible light, though relatively weak, are highly de-

pendent on the chosen preparation methods [9]. One issue that arises is the significant disparity in photoresponse between visible light and UV irradiation. Thus, it is imperative to create and enhance a novel photoresponsive nanostructure of TiO_2 that can effectively harness visible light, while possessing also improved surface characteristics and exceptional chemical and physical stability. This is essential for the widespread adoption of photovoltaic systems in various commercial applications.

Various techniques have been employed to create films of nanostructures made of metal oxides, such as TiO_2 [10]. These methods include sol–gel spin coating, chemical bath deposition, reactive sputtering, pulsed-laser deposition, and chemical vapour deposition [11, 12]. The sol–gel spin coating technique has become a popular choice for nano-TiO_2 fabrication due to its ability to produce samples with a consistent synthetic approach, resulting in a highly efficient UV–Vis optical response [13]. For this project, TiO_2 is created using a sol–gel spin coating method and applied onto borosilicate glass substrates. The process involves utilizing titanium tetraisopropoxide, isopropanol, acetic acid, and deionized water as the initial components. Through precise manipulation of the ratio of precursor materials to solvent, along with a pH of 9.5 achieved by using nitric acid, a consistent and transparent sol of TiO_2 colloidal suspension in the nanometer scale was obtained. This sol was then applied onto meticulously cleaned borosilicate glass substrates and spun at a speed of 4000 revolutions per minute for 30 seconds using suction.

TiO_2 nanostructure films fabricated by sol–gel spin coating have excellent optical properties suitable for application in solid-state photovoltaic solar cells. Optical characteristics of TiO_2 films under visible light though are very weak, but they strongly depend on preparation methods. The main problem is that photoresponse under visible light is much lower than that under UV irradiation. Therefore, the development of new and optimized photoresponsive TiO_2 nanostructure for the existing optical properties exhibiting activity upon visible light with surface characteristics of improved performance, and of the high chemical and physical stability are crucial for broader scale utilization of photovoltaic systems in commercial applications.

Transparent metal oxide (TiO_2) thin films find applications in a wide range of fields, including optoelectronics, energy efficiency, sensors, and antireflective coatings; their unique properties make them an essential component of many modern technologies [14, 15], especially, in one of the promising applications such as windows of solar cells. Thin TiO_2 films are commonly used as a UV-blocking layer in solar cells due to their high refractive index, high trans-

parency in the visible range, and strong absorption of ultraviolet (UV) light [16]. The mechanism behind this lies in the fact that TiO_2 is a wide-band gap semiconductor with a band gap of approximately 3.2 eV, which makes it highly transparent in the visible range but highly absorbing in the UV range. When UV light is incident on the TiO_2 layer, the photons with energy more significant than the band gap of TiO_2 are absorbed by the material, causing electrons to be excited from the valence band to the conduction band. These excited electrons generate electron–hole pairs, which can recombine radiatively or non-radiatively. However, the thickness of the TiO_2 layer is appropriate. In that case, most of the UV light is absorbed within the TiO_2 layer, reducing the UV-light amount that reaches the underlying solar cell layers [17, 18].

TiO_2 thin films can also act as a scattering layer, reducing the amount of UV light that reaches the underlying solar cell layers. The scattering effect is due to the refractive index mismatch between TiO_2 and the surrounding medium, which causes light to be scattered at the interface, which leads to an increase in the optical path length of the light, which results in a reduction in the amount of light that reaches the underlying solar cell layers [18, 19].

Thin films are one of the essential branches of solid-state physics, especially, semiconductors' thin films, because of their wide applications in many electrical, electronic, and optical fields. The thin film could be condensed from atoms, ions, or molecules to construct a single layer or multilayers on a solid surface (metal or glass substrate), depending on the application needed [20]. Recently, researchers have been interested in thin films, and they focused their research on developing methods for preparing them by various techniques due to the importance of thin films in a wide range of applications such as electronics, optics, and electrooptics, surface modifications (hydrophobic and anticorrosion surfaces). Thin films can be deposited by many methods and techniques based on physical or chemical mechanisms according to the application needed. Thin-film deposition techniques are divided into two parts, depending on whether chemical changes occurred in the materials used to prepare the thin films [21, 22]. Sol–gel is one of the most widely used methods for depositing thin films of TiO_2 due to several advantages due to its low-temperature deposition, high purity, easy thickness control, large-area deposition, and cost-effectiveness [23, 24]. The thin-film deposition process requires special techniques; the spin coater technique has been used in current research.

2. EXPERIMENTAL WORK

Firstly, each glass substrate was cleaned by dipping it in ethanol

TABLE 1. The thicknesses for each sample measured by optical ellipsometry.

Annealed samples	Thickness, nm
TiO_2 at 360°C	24.69
TiO_2 at 460°C	23.34
TiO_2 at 550°C	25.69
TiO_2 at 700°C	24.50

for 20 minutes inside the ultrasonic bath and then kept in acetone. After drying them with nitrogen gas, the substrate would be ready for use. The sol–gel phase was formed by adding 3.15 ml of titanium isopropoxide as precursor material to 30 ml of absolute ethanol; the components' mixture was magnetically stirred for around 20 minutes under room temperature ($\cong$ 30°C), through which 5 ml of glacial-acetic acid was added as a catalyst after 20 minutes yellowish transparent solution has been formed. The chemical equation $C_{12}H_{28}O_4Ti + 6C_2H_5OH \rightarrow TiO_2 + 8(CH_3)_2CHOH$ illustrates the chemical reaction.

All materials used were supplied with high purity. The final step is depositing a thin film; this step is done by dropping the prepared solution on the cleaned substrate and coating it with a rotation speed of 3000 rpm. Obtained films were dried at a temperature of $\cong$ 60°C before sintering them at different temperatures, 360°C, 460°C, 550°C, and 700°C, by using the programmed oven for 50 minutes for all films; the thickness of these films was measured by optical ellipsometry n, and k as well as.

3. RESULT AND DISCUSSIONS

3.1. Ellipsometry (n, k, d)

The relationship between (n, k, d) and annealing temperatures for TiO_2 thin films is complex and depends on multiple factors. Ellipsometry can be a valuable tool to characterize the optical properties of the films and monitor changes induced by annealing temperatures depending on various factors such as the deposition method, substrate, and annealing conditions [25].

Ideally, as the annealing temperature increases, the thickness of the TiO_2 film may decrease due to evaporation or diffusion of atoms; this can lead to a decrease in refractive indices and an increase in k, but that arranged relationships did not accrue with all samples measured as shown in Figs. 1, 2. These behaviours can be attributed to structural changes in the film with annealing temperatures and leading to variations in the refractive index and extinction coeffi-

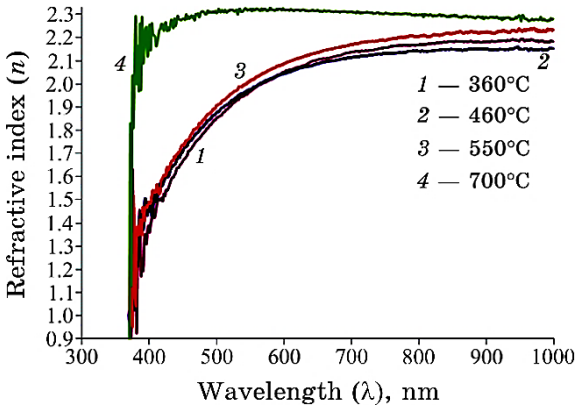

Fig. 1. The relationships between refractive index and wavelengths as measured by ellipsometry.

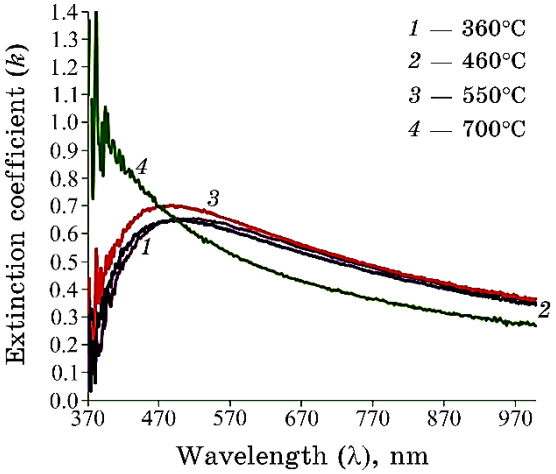

Fig. 2. The behaviours of the extinction coefficient as a function of wavelength.

cient. However, the good thing about these thin films is that we obtained essential values for the refractive index at annealing temperatures of 360, 460 and 500°C. The most suitable and best film for optical applications was the film annealed at 500°C due to refractive index values of 1.48–2.2 at the visible range [26].

A visual representation is shown depicting the reflection of light off the surface of a sample. The vectors labelled **s** and **p** denote the orientation of polarized light determined by the plane of incidence. The angle, at which the light strikes the surface, is represented by ϕ, and the refractive indices of the surrounding environment, film layer, and sub-

strate are represented as N_0, N_f, and N_s, respectively (G. E. Jellison Jr., in *Encyclopedia of Spectroscopy and Spectrometry* (1999)):

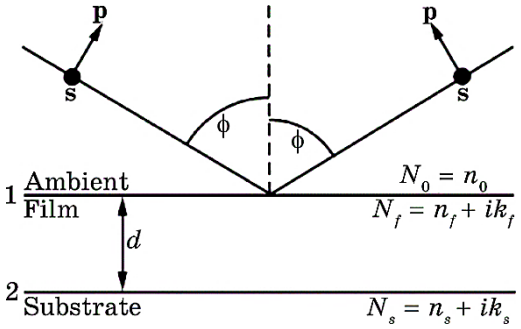

3.2. Optical Absorbance and Transmittance

The relationship between the optical absorption and transmittance of TiO_2 and the annealing temperature depends on the wavelength of the incident light, which determines the region of the electromagnetic spectrum being considered.

TiO_2 typically exhibits high absorption and low transmittance within the UV region, attributed to Ti^{3+} states and oxygen vacancies. As the annealing temperature is increased, the concentrations of these defects decrease, resulting in a decrease in absorption and an increase in transmittance, as shown in Figs. 3, 4, *a* [27, 28].

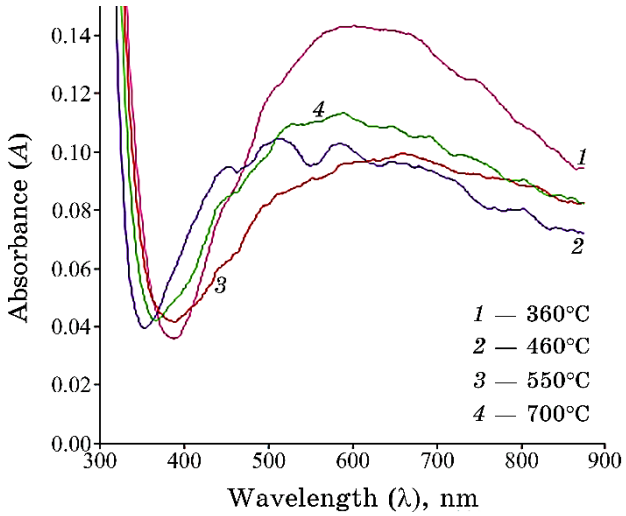

Fig. 3. Optical absorbance of TiO_2 films with different annealing temperatures.

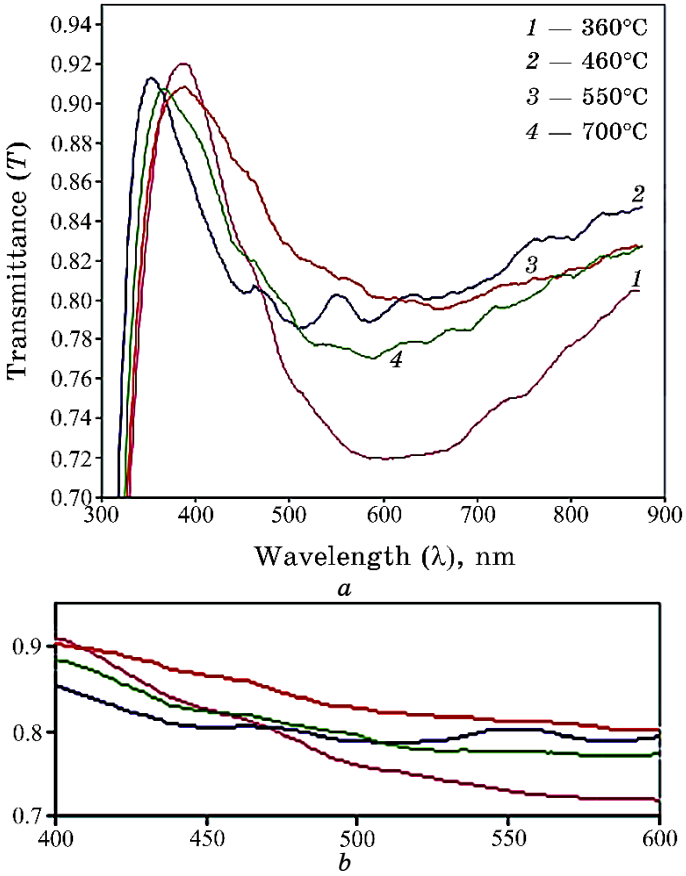

Fig. 4. (*a*) Optical transmittance spectrum of TiO_2 films with different annealing temperatures; (*b*) optical transmittance spectrum within the visible region.

Within the visible region, TiO_2 typically exhibits low absorption and high transmittance, which is attributed to the band-gap absorption of TiO_2 (see Fig. 4, *b*). As the annealing temperature increases, the band gap of TiO_2 increases, resulting in a slight shift of the absorption edge to higher energies, hence a decrease in absorption, and an increase in transmittance [29].

Generally, the relationship between optical absorption and transmittance of TiO_2 with annealing temperature is complex. It depends on several factors, such as the crystal structure, morphology, size of the TiO_2 particles, and the experimental conditions. However, in general, the optical properties of TiO_2 can be tailored by controlling the annealing temperature, which makes it a valuable material for a wide range of applications, including UV block layers such as solar

cell windows, protecting glasses, and photosensors at a certain spectrum. The best values of optical transmittance were obtained from the annealed film at 500°C; the red curve in Fig. 4 shows the largest transmittance of the visible length, reaching between 80% and 90% at wavelengths ranging from 400 to 600 nm, respectively. This film can be used in UV block layers, the most important of which are windows for solar cells and in medical glasses [29–31].

3.3. Reflectance and Refractive Index

TiO_2 thin films exhibit reflectance and refractive index variations based on factors like film thickness, wavelength of light, and annealing temperature. The reflectance of TiO_2 films can be adjusted by manipulating the refractive index and thickness. Interference effects occur when the film thickness is comparable to the wavelength, resulting in constructive or destructive interference and changes in reflectance. The refractive index of TiO_2 films is high in the visible and UV regions and can be increased by increasing film thickness or annealing at higher temperatures. The refractive index also varies with the wavelength of light due to dispersion effects. The film thickness affects interference effects, with thinner films showing lower reflectance and thicker films exhibiting higher reflectance due to multiple internal reflections. Annealing temperature influences the film crystallinity and density, affecting its refractive index and optical properties.

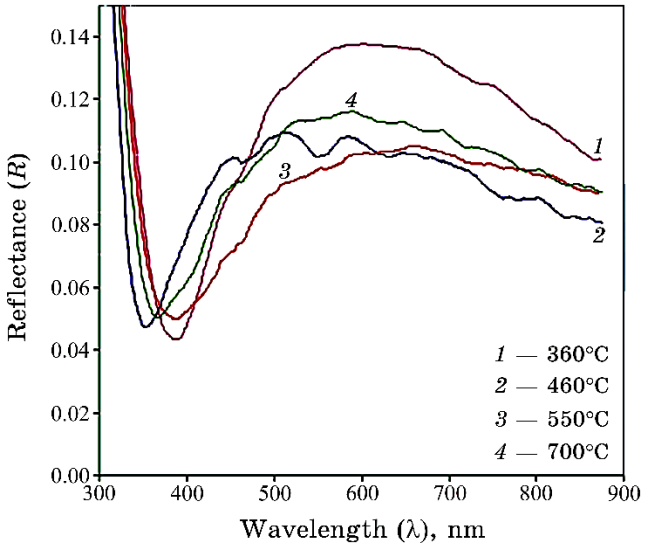

Fig. 5. Reflectance (R) of TiO_2 thin films.

TABLE 2. The important values of some optical properties within the wavelength interval 400–700 nm.

Temperature, °C	Absorption (A)	Transmittance (T)	Reflectance (R)	Thickness, nm	Extinction coefficient (k)	Refractive index (n)
360	0.037–0.136	0.918–0.730	0.044–0.132	24.69	0.109–0.706	1.281–2.364
460	0.059–0.096	0.872–0.801	0.068–0.102	23.34	0.187–0.529	1.442–1.793
500	0.044–0.097	0.903–0.799	0.052–0.103	25.69	0.125–0.485	1.333–1.778
700	0.050–0.105	0.891–0.784	0.058–0.11	24.5	0.149–0.552	1.377–1.879

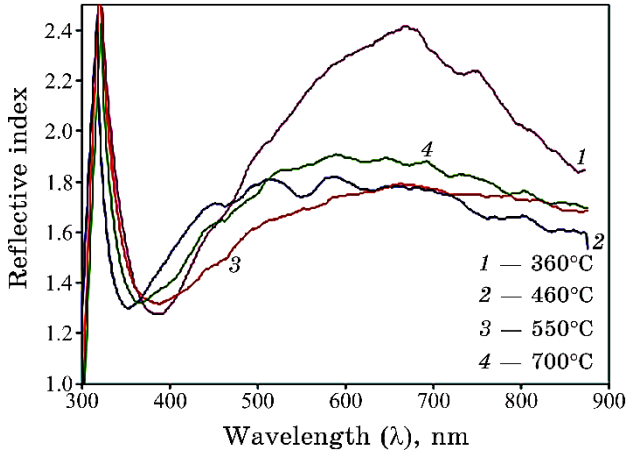

Fig. 6. The refractive index (n) of TiO_2 thin films.

Higher annealing temperatures generally increase the refractive index by improving crystallinity and reducing porosity. By controlling these parameters, the optical properties of TiO_2 thin films can be tailored for specific applications [32, 33].

The best value of reflectance and refractive index appears for the films annealed at 460°C and 500°C, as the films showed low reflectance values in the visible region 400–700 nm. It should be noted that the annealed film at a temperature of 500°C is the best, allowing visible light transmittance; this property is essential in both solar-cell window applications and UV-block ones.

3.4. The Band Gap E_g

$$(\alpha h\nu) = A(h\nu - E_g)^m; \tag{1}$$

here, A is a constant that depends on the electron–hole mobility; α is an absorption coefficient, cm^{-1}; $h\nu$ is photon energy (E_v); $m = 1/2$ for a direct band gap:

$$(\alpha h\nu) = A(h\nu - E_g)^{1/2}; \tag{2}$$

$m = 2$ for an indirect band gap.

Figure 7 shows the linear proportion between $(\alpha h\nu)^{1/2}$ and $h\nu$ of annealed samples; it also seems that there is no apparent regularity in the values of the optical energy gaps with the relationship with annealing temperatures, which may be due to several reasons, the most important of which is the thicknesses of thin films, or perhaps

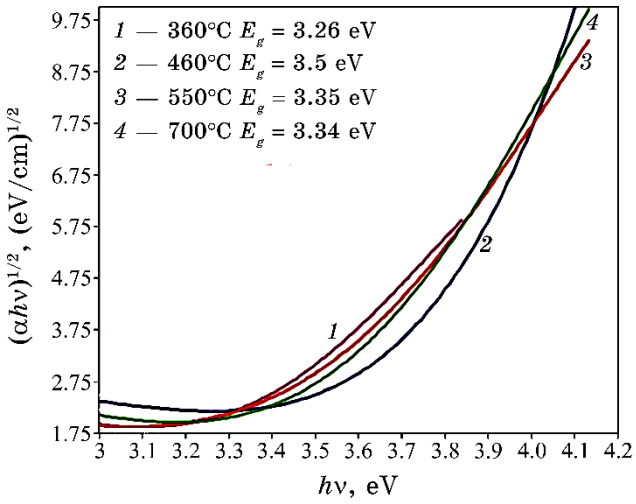

Fig. 7. The band gap of TiO_2 thin films.

the non-uniformity of the coats as well as [34].

TiO_2 thin films have high optical transparency in the visible range and a wide band gap of ≅ 3.2 eV, as obtained for all samples prepared, especially at $T = 500$°C, which has n and R, making it ideal for use as a window layer in solar-cell applications [35]. The high transparency ensures that the solar cell absorbs the maximum amount of light. The wide band gap of TiO_2 also ensures that the generated charge carriers can be efficiently extracted from the cell. The range of 2.3–2.5 is higher than that of most other transparent conducting oxides, making them suitable for antireflective coatings [36, 37].

4. CONCLUSION

According to the results and interpretations, which were stated in the research, we reached the following conclusions.

The values of optical transmittance obtained from the annealed film at 500°C were the best, as we can see in Fig. 4; the red curve showed the largest transmittance of the visible length, reaching between 80% and 90% at wavelengths ranging from 400–600 nm, respectively. This film can be used in UV block layers, the most important of which are windows for solar cells, as well as in medical glasses; and the band gap of TiO_2 thin film annealed at 500°C was the best.

The best reflectance and refractive index values appear in the films annealed at 460°C and 500°C, as the films showed low reflec-

tance values in the visible region 400–700 nm. It should be noted that the annealed film at a temperature of 500°C is the best, allowing visible light transmittance; and this property is essential in solar-cell window applications and UV-block applications.

REFERENCES

1. M. Pelaez, N. T. Nolan, S. C. Pillai, M. K. Seery, P. Falaras, A. G. Kontos, P. S. Dunlop, J. W. Hamilton, J. A. Byrne, K. O'shea, and M. H. Entezari, *Appl. Catal. B: Environ.*, **125**, No. 1: 331 (2012); https://doi.org/10.1016/j.apcatb.2012.05.036
2. B. Al-Zubaidy, N. S. Radhi, and Z. S. Al-Khafaji, *Int. J. Mech. Eng. Technol.*, **10**, No. 1: 776 (2019); https://cdnx.uobabylon.edu.iq/research/repository1_publication14452_28_816.pdf
3. S. Sattar, Y. Alaiwi, N. S. Radhi, and Z. Al-Khafaji, *Acad. J. Manuf. Eng.*, **21**, No. 4: 86 (2023); https://ajme.ro/current_issue.php
4. Sabaa Sattar, Yaser Alaiwi, Nabaa Sattar Radhi, Zainab Al-Khafaji, Osamah Al-Hashimi, Hassan Alzahrani, and Zaher Mundher Yaseen, *J. King Saud Univ. Sci.*, **35**, No. 8: 102861 (2023); doi:10.1016/j.jksus.2023.102861
5. Mauricio E. Calvo, José R. Castro Smirnov, and Hernán Míguez, *J. Polym. Sci. Part B: Polym. Phys.*, **50**, Iss. 14: 945 (2012); https://doi.org/10.1002/polb.23087
6. Nabaa S. Radhi, Ahlam Hamid Jasim, Zainab S. Al-Khafaji, and Mayadah Falah, *Nanosistemi, Nanomateriali, Nanotehnologii*, **21**, Iss. 4: 769 (2023); https://doi.org/10.15407/nnn.21.04.769
7. S. Ghosh and A. P. Das, *Toxicol. Environ. Chem.*, **97**, No. 5: 491 (2015); https://doi.org/10.1080/02772248.2015.1052204
8. Natarajan Shanmugam, Rishi Pugazhendhi, Rajvikram Madurai Elavarasan, Pitchandi Kasiviswanathan, and Narottam Das, *Energies*, **13**, Iss. 10: 2631 (2020); https://doi.org/10.3390/en13102631
9. H. A. Sallal, M. S. Radhi, M. H. Mahboba, and Z. Al-Khafaji, *Egypt. J. Chem.*, **55**, No. 6: 197 (2023); doi:10.21608/EJCHEM.2022.154630.6684
10. Chen Yang, Huiqing Fan, Yingxue Xi, Jin Chen, and Zhuo Li, *Appl. Surf. Sci.*, **254**, Iss. 9: 2685 (2008); https://doi.org/10.1016/j.apsusc.2007.10.006
11. M. N. Chaudhari, R. B. Ahirrao, and S. D. Bagul, *IJRASET*, **9**, No. 1: 5215 (2021); https://www.ijraset.com/fileserve.php?FID=36154
12. N. D. Fahad, N. S. Radhi, Z. S. Al-Khafaji, and A. A. Diwan, *Heliyon*, **9**, No. 3: 14103 (2023); https://doi.org/10.1016/j.heliyon.2023.e14103
13. I. Karaduman Er, S. Uysal, A. Ateş, and S. Acar, *J. Mater. Sci. Mater. Electron.*, **34**, No. 20: 1512 (2023); https://doi.org/10.1007/s10854-023-10930-9
14. X. Yu, T. J. Marks, and A. Facchetti, *Nat. Mater.*, **15**, No. 4: 383 (2016); https://doi.org/10.1038/nmat4599
15. Timothy J. Coutts, Thomas O. Mason, John D. Perkins, and David S. Ginley, *Proc. Electrochem. Soc.*, **99**, No. 1999: 274 (1999); https://docs.nrel.gov/docs/fy99osti/26640.pdf
16. Jianyu Fu, Wenjuan Xiong, Haiping Shang, Ruiwen Liu, Junfeng Li, Weibing Wang, Wenwu Wang, and Dapeng Chen, *Mater. Sci. Semicond. Process*, **89**,

No. 1: 1 (2019); https://doi.org/10.1016/j.mssp.2018.08.024
17. S. M. Sze and K. K. Ng, *Physics of Semiconductor Devices* (John Wiley & Sons, Inc.: 2006); https://doi.org/10.1002/0470068329
18. Bing Zhou, Xiaohong Jiang, Zhubo Liu, Ruiqi Shen, and Aleksandr V. Rogachev, *Mater. Sci. Semicond. Process*, **16**, No. 2: 513 (2013); https://doi.org/10.1016/j.mssp.2012.05.001
19. S. H. Woo and C. K. Hwangbo, *Surf. Coat. Technol.*, **201**, Nos. 19–20: 8250 (2007); https://doi.org/10.1016/j.surfcoat.2006.01.085
20. H. S. Nalwa, *Handbook of Thin Films (Five-Volume Set)* (Academic Press: 2001).
21. X. Tian, X. Cui, T. Lai, J. Ren, Z. Yang, M. Xiao, B. Wang, X. Xiao, and Y. Wang, *NMS*, **3**, No. 4: 390 (2021); https://doi.org/10.1016/j.nanoms.2021.05.011
22. N. K. Elumalai, M. A. Mahmud, D. Wang, and A. Uddin, *Energies*, **9**, No. 11: 861 (2016); https://doi.org/10.3390/en9110861
23. T. Wen, J. Gao, J. Shen, and Z. Zhou, *J. Mater. Sci.*, **36**, No. 1: 5923 (2001); https://doi.org/10.1023/A:1012989012840
24. E. Traversa, G. Gnappi, A. Montenero, and G. Gusmano, *Sens. Actuators B: Chem.*, **31**, Nos. 1–2: 59 (1996); https://doi.org/10.1016/0925-4005(96)80017-7
25. Robert Alan May, *Ellipsometric and Nanogravimetric Porosimetry Studies of Nanostructured, Mesoporous Electrodes* (Dissertation for Doctor of Philosophy) (The University of Texas at Austin: 2009).
26. F. Scheepers, A. Stähler, M. Stähler, M. Carmo, W. Lehnert, and D. Stolten, *JCTR*, **16**, No. 1: 1213 (2019); https://doi.org/10.1007/s11998-019-00206-5
27. J. Ben Naceur, M. Gaidi, F. Bousbih, R. Mechiakh, and R. Chtourou, *Curr. Appl. Phys.*, **12**, Iss. 2: 422 (2012); https://doi.org/10.1016/j.cap.2011.07.041
28. X. Zhang, Y. Zhang, Y. Wang, Q. Wang, Z. Liu, R. Geng, H. Wang, W. Jiang, and W. Ding, *J. Alloys Compd.*, **929**, No. 1: 167278 (2022); https://doi.org/10.1016/j.jallcom.2022.167278
29. S. Banerjee, E. Adhikari, P. Sapkota, A. Sebastian, and S. Ptasinska, *Mater.*, **13**, No. 13: 2931 (2020); https://doi.org/10.3390/ma13132931
30. Yu-Hsiang Wang, Kazi Hasibur Rahman, Chih-Chao Wu, and Kuan-Chung Chen, *Catalysts*, **10**, No. 6: 598 (2020); https://doi.org/10.3390/catal10060598
31. N. Mozaffari, S. H. Elahi, S. S. Parhizgar, N. Mozaffari, and S. M. Elahi, *MRX*, **6**, No. 11: 116428 (2019); doi:10.1088/2053-1591/ab4662
32. Fubao Zhang, Xianming Wang, Haonan Liu, Chunli Liu, Yong Wan, Yunze Long, and Zhongyu Cai, *Applied Sciences*, **9**, No. 12: 2489 (2019); https://doi.org/10.3390/app9122489
33. V. T. Lukong, K. Ukoba, and T. C. Jen, *Int. J. Adv. Manuf. Technol.*, **122**, Nos. 9–10: 3525 (2022); https://doi.org/10.1007/s00170-022-10043-3
34. J. I. Larruquert, *Optical Properties of Thin Film Materials at Short Wavelengths. Optical Thin Films and Coatings* (Elsevier: 2018), p. 291–356; doi:10.1016/B978-0-08-102073-9.00007-2
35. X. Teng, B. Liu, and T. Ichiye, *Chem. Phys.*, **153**, No. 10 (2020); doi:10.1063/5.0021472
36. A. J. Haider, A. A. Najim, and M. A. H. Muhi, *Opt. Commun.*, **370**, No. 1: 263 (2016); doi: 10.1016/j.optcom.2016.03.034
37. O. Y. Ramírez-Esquivel, D. A. Mazón-Montijo, Z. Montiel-González, and F. S. Aguirre-Tostado, *Sol. Energy Mater. Sol. Cells*, **185**: 392 (2018); https://doi.org/10.1016/j.solmat.2018.05.029